

# RSC Advances



This is an *Accepted Manuscript*, which has been through the Royal Society of Chemistry peer review process and has been accepted for publication.

*Accepted Manuscripts* are published online shortly after acceptance, before technical editing, formatting and proof reading. Using this free service, authors can make their results available to the community, in citable form, before we publish the edited article. This *Accepted Manuscript* will be replaced by the edited, formatted and paginated article as soon as this is available.

You can find more information about *Accepted Manuscripts* in the [Information for Authors](#).

Please note that technical editing may introduce minor changes to the text and/or graphics, which may alter content. The journal's standard [Terms & Conditions](#) and the [Ethical guidelines](#) still apply. In no event shall the Royal Society of Chemistry be held responsible for any errors or omissions in this *Accepted Manuscript* or any consequences arising from the use of any information it contains.

# Clusters protected with mixed proteins exhibiting intense photoluminescence

Jyoti Sarita Mohanty,<sup>‡</sup> Ananya Baksi,<sup>‡</sup> Haiwon Lee and T. Pradeep\*

<sup>1</sup>DST Unit of Nanoscience (DST UNS), and Thematic Unit of Excellence (TUE),

Department of Chemistry, Indian Institute of Technology Madras, Chennai - 600 036, India

<sup>2</sup>Department of Chemistry, Institute of Nanoscience and Technology, Hanyang University, Seoul- 133-791, Korea.

<sup>‡</sup> Contributed equally

## Abstract

Here we report the synthesis and detailed mass spectrometric and spectroscopic characterization of highly luminescent gold and silver clusters protected with mixed proteins. Taking advantage of the aggregation tendency of the protein, lysozyme (Lyz), we could make an inter-protein conjugate from a physical mixture of the two proteins, bovine serum albumin (BSA) and Lyz. Based on the matrix assisted laser desorption ionization mass spectrometry (MALDI MS) data, the new cluster is assigned as  $\sim\text{Au}_{36}@\text{BSA-Lyz}$ . This specific system showed very high red luminescence and the calculated quantum yield was 42% which is highest till date for such cluster systems. A similar study on silver system showed the formation of  $\sim\text{Ag}_{35}@\text{BSA-Lyz}$  when similar metal and protein concentration was used. By varying the concentration of the silver precursor, different compositions of the cluster protected by the mixed protein have been achieved. Such a system with high quantum yield can be used for various applications such as sensors for ultralow levels of analytes, fluorescent tags and for tracking biomolecules in real systems.

## 1. Introduction

Noble metal nanoclusters are one of the most fascinating research areas of contemporary materials science.<sup>1-5</sup> Several metals have been used in this context among which gold and silver have drawn maximum attention. Most of the cluster chemistry is concentrated with monolayer protected clusters. Thiol ligands are of larger interest as the Au-S bond is strong and by changing the ligand (thiol), one can play with the properties of the clusters. Many thiol protected gold and silver clusters have been reported and some of them have been crystallized. Examples include,  $\text{Au}_{25}(\text{SR})_{18}$ ,<sup>6, 7</sup>  $\text{Au}_{30}\text{S}(\text{SR})_{18}$ ,<sup>8</sup>  $\text{Au}_{38}(\text{SR})_{24}$ ,<sup>9</sup>  $\text{Au}_{36}(\text{SR})_{24}$ ,<sup>10</sup>  $\text{Au}_{102}(\text{SR})_{44}$ ,<sup>11</sup> and  $\text{Ag}_{44}(\text{SR})_{30}$ .<sup>12, 13</sup> Three types of modifications are possible on such monolayer protected clusters; i) ligand exchange<sup>14-16</sup>, ii) alloying<sup>12</sup> of the core and iii) both the above top varying degree simultaneously. Both of these have been studied in detail for monolayer protected gold clusters. Some of these chemically modified clusters have been crystallized.<sup>12</sup>

Macromolecular templates are another platform for synthesizing such clusters.<sup>4, 17, 18</sup> DNA,<sup>19</sup> dendrimer<sup>20</sup> and most recently proteins<sup>21</sup> have been used as templates for cluster formation. Most often used proteins are bovine serum albumin (BSA),<sup>21-28</sup> human serum albumin (HSA),<sup>29, 30</sup> lactoferrin (Lf),<sup>31, 32</sup> lysozyme (Lyz),<sup>33-36</sup> insulin,<sup>37</sup> etc. Major characterization methods of such clusters involve mass spectrometry; mainly matrix assisted laser desorption and ionization (MALDI)<sup>21, 25, 27-29, 31, 34, 38</sup> as none of these clusters could be crystallized so far. General synthetic route of such clusters involve adduct formation between the protein and the metal and subsequent reduction of the ion to the M(0) state at elevated pH.<sup>21, 31</sup> During the core formation, inter-protein metal ion transfer takes place which leads to the regeneration of the free protein. As the core evolves to a bigger size, more and more free protein regeneration can be seen.<sup>31</sup> Variety of cores have been reported depending on the size and structure of the protein.<sup>31, 34</sup> For smaller proteins like Lyz, core compositions have been confirmed from the

aggregates (formed via inter-protein interaction through salt-bridge).<sup>34</sup> For a single protein, by changing experimental conditions and using different parameters, one can modify the core size as shown in a recent study by predefining the protein structure at specific pH.<sup>38</sup> Different methods have been tried for modifying the core and shell composition such as core etching,<sup>23</sup> sonochemical method,<sup>39</sup> microwave synthesis,<sup>40, 41</sup> slow reduction by carbon monoxide,<sup>38</sup> etc. Such clusters exhibit intense luminescence which is highly sensitive to the presence of foreign elements which can interact and quench the luminescence.<sup>2</sup> This luminescence property has been applied for sensing metal ions<sup>24, 26, 33, 40</sup> and small molecules,<sup>30, 42-48</sup> as well as *in-vitro* and *in-vivo* imaging and labelling.<sup>23, 49</sup> A few of the proteins are known to retain biological activity even after cluster formation,<sup>37</sup> indicating that the protein remains as such and the cluster formation does not occur *via* the involvement of the active site of the protein. Presence of another protein might help in enhancing the Fröster resonance energy transfer (FRET) probability and hence the quantum yield may be increased. This could be possible following the ligand exchange procedure used for monolayer protected clusters where after ligand exchange, properties of both the ligands can be monitored. Nihorii *et al.* have separated all the ligand exchanged products of  $\text{Au}_{25}(\text{SR}_1)_{18-x}(\text{SR}_2)_x$  ( $x = 0, 1, 2, \dots, 18$ ) by chromatography and characterized them by mass spectrometry.<sup>16</sup> Supramolecular chemistry of such clusters *via* ligand exchange by thiolated calixarene has been studied in detail.<sup>14</sup> Taking advantage of ligand and cyclodextrin inclusion complex formation, Mathew *et al.* have recently shown that supramolecular chemistry is possible for such  $\text{Au}_{25}(\text{SR})_{18}$  clusters.<sup>15</sup> Exchanging the core by other metals can also enhance the physico-optical properties significantly as shown by Wang *et al.* where they have exchanged Ag with Au and obtained 200-fold increments in the luminescence (41% quantum yield).<sup>50</sup>

There are reports of ligand exchange and mixed ligand protection for monolayer protected clusters. Recently, ligand exchange of  $\text{Au}_{25}(\text{SR})_{18}$  was separated using high performance

liquid chromatography (HPLC) and each of the exchanged products were observed using MALDI MS.<sup>16</sup> Although mixed protein matrix like egg shell membrane<sup>46</sup> and hair fibre<sup>44</sup> are used for cluster synthesis, none of these clusters could be characterized to get an idea about the precise core size. Proteins are macromolecules and they behave differently than small thiol ligands. Protein-protein interaction has been studied by biologists which has strong biological implications. This kind of interaction is very specific and occurs only between specific proteins. Following the ligand exchange of monolayer protected clusters, the effect of addition of external protein on a preformed protein protected cluster was observed in this report.

Most of the reports have claimed that the luminescence of protein protected clusters is due to FRET between the protein and the cluster.<sup>4, 32</sup> Compared to monolayer protected gold clusters, protein protected clusters have higher quantum yield but the yield is still not very promising unlike the fluorescent dyes (15% for protein protected clusters whereas dyes show more than 95%). Keeping this in mind, an attempt to ligand exchange protein protected clusters was made, where we hoped to see different properties by protein exchange. More interestingly, we expected to be in a position to regulate the properties of the proteins as well as the cluster core.

Here we report, the formation of highly fluorescent gold quantum clusters with the highest quantum yield (42.4%) in a mixed protein system. Two differently sized proteins namely, BSA and Lyz have been used for this study and the reactants as well as the products have been probed by mass spectrometry and optical spectroscopic techniques. A new cluster core, Au<sub>36</sub> protected with both BSA and Lyz was obtained with a four-fold increase in the fluorescence intensity which leads to 42.4% quantum yield for this system.

## 2. Experimental

### 2.1. Reagents and materials

Bovine serum albumin (BSA) at pH 6-7 was purchased from SRL Chemical Co. Ltd., India. Lysozyme and sinapic acid were purchased from Sigma Aldrich. Tetrachloroauric acid trihydrate ( $\text{HAuCl}_4 \cdot 3\text{H}_2\text{O}$ ) was purchased from CDH, India. Silver nitrate ( $\text{AgNO}_3$ ) and sodium hydroxide ( $\text{NaOH}$ ) were purchased from Rankem, India. Sodium borohydride ( $\text{NaBH}_4$ ) was purchased from Spectrochem, India. All the chemicals were used without further purification. MilliQ water was used for all the experiments.

### 2.2. Instrumentation

Luminescence measurements were carried out using a Jobin Yvon NanoLog instrument. Both the excitation and emission spectra were collected with a band pass of 3 nm. MALDI MS studies were performed using a Voyager DE PRO Biospectrometry Workstation from Applied Biosystems. A pulsed nitrogen laser of 337 nm was used for the MALDI MS studies. Mass spectra were collected in linear positive mode and an average of 250 shots was used for each spectrum. High resolution transmission electron microscopy (HRTEM) was performed with a JEOL 3010, a 300 kV instrument, equipped with an ultra high resolution (UHR) polepiece. Sample for HRTEM was prepared by dropping the dispersion on a carbon coated copper grid. Scanning electron microscopy (SEM) and energy dispersive analysis of the X-ray (EDAX) images were collected by using an FEI QUANTA-200 SEM. Samples were spotted on an indium tin oxide (ITO) conducting glass substrate and dried in ambient condition for SEM and EDAX measurements. X-Ray photoelectron spectroscopy (XPS)

studies were carried out with an Omicron ESCA probe spectrometer with polychromatic Mg K $\alpha$  X-rays ( $h\nu = 1253.6$  eV). The samples were spotted as drop cast films on a sample stub.

### 2.3. Synthesis

BSA and Lyz were mixed in 1:1 molar ratio and stirred for 10 min. To this 1 mL 6 mM HAuCl<sub>4</sub> was added. The solution was stirred for another 15 min. Further, to this mixture, 100  $\mu$ L of 1 M NaOH was added and stirred for 12 h to get a clear brown solution. All the samples were taken directly from the reaction mixture for MALDI MS and other characterization studies. Ag clusters were prepared keeping protein and Ag concentration exactly the same as used for Au cluster synthesis. In this case, NaBH<sub>4</sub> was used as the external reducing agent.

## 3. Results and Discussion

### 3.1. Gold cluster formation in mixed protein matrix

Monolayer as well as protein protected gold and silver clusters were studied extensively.<sup>1, 3, 17</sup> Protein protected clusters are typically synthesized by mixing a preferred ratio of protein and metal ion to form a metal bound protein adduct and subsequent reduction of the adducts at basic condition (pH 12). At this pH, protein unfolds (seen in circular dichroism)<sup>27, 31, 32, 34</sup> and disulfide bonds between the cysteine residues break. In a system containing two different proteins, inter protein disulfide bonds may create new inter-protein adducts. Different type of possibilities can be thought of as i) large protein-large protein, ii) large protein-small protein and iii) small protein-small protein. In this report, the first two possibilities were studied. Lf, a large protein of 83 kDa mass and Lyz, a small protein of 14.3 kDa mass were chosen in combination with BSA to study the exchange.

Isolated gold and silver clusters protected with BSA<sup>25, 27</sup> as well as Lyz<sup>34</sup> have been characterized thoroughly by several spectroscopic and mass spectrometric tools. They show well defined mass spectral signatures as observed in MALDI MS. Core size of such clusters is assigned by considering the mass shift from the parent protein after cluster formation. In most of the cases, core size depends on the concentration of protein and metal ion in the solution and varies linearly with metal concentration. At a specific Au<sup>3+</sup> concentration,  $\sim\text{Au}_{30}\text{@BSA}^{27}$  forms (1:16 BSA:Au<sup>3+</sup> molar concentration), whereas an Au<sub>10</sub> core is observed for Lyz (1:4 Lyz:Au<sup>3+</sup> molar concentration).<sup>34</sup>

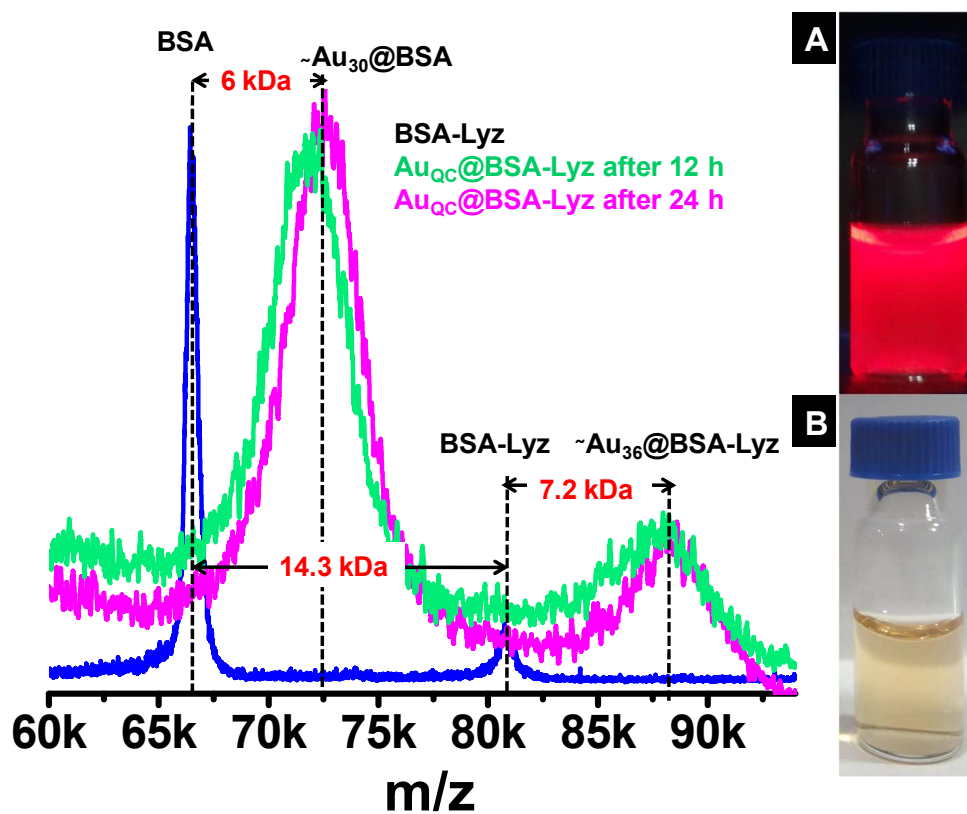


**Fig. 1.** Comparative MALDI MS of BSA-Lyz and Au<sub>QCs</sub>@BSA-Lyz in linear positive mode showing the presence of  $\sim\text{Au}_{36}\text{@BSA-Lyz}$  peak at m/z 88.3 kDa in case of a protein mixture, which was not present in the case of gold clusters protected either by BSA or Lyz. Inset shows the photographs of  $\sim\text{Au}_{36}\text{@BSA-Lyz}$  under UV A) and visible light B), respectively.



We have used a physical mixture of 1:1 (75  $\mu\text{M}$ ) BSA and Lyz and incubated the mixture in presence of 6 mM  $\text{Au}^{3+}$  for a few minutes to allow reduction of  $\text{Au}^{3+}$  to  $\text{Au}^+$  by aromatic amino acids of the proteins and subsequently NaOH was added. Formation of clusters was confirmed from the appearance of slight red luminescence under UV light after 4 h of incubation. We have further incubated the mixture up to 12 h to allow the complete conversion of  $\text{Au}^+$  to  $\text{Au}^0$ . Fig. 1 shows the comparison of MALDI MS spectra of BSA-Lyz and  $\text{Au}_{\text{QC}}@\text{BSA-Lyz}$  in linear positive ion mode. In the 60-100 kDa mass range, BSA-Lyz mixture showed three peaks corresponding to  $\text{BSA}^+$ ,  $\text{BSA-Lyz}^+$  and  $\text{BSA-Lyz}_2^+$  (see below for details). During cluster formation, a new peak appeared at 88.3 kDa along with  $\sim\text{Au}_{30}@\text{BSA}$  at 72 kDa (Fig. S1 for MALDI MS of  $\sim\text{Au}_{30}@\text{BSA}$ ). Corresponding +2 charge species was observed at 44.1 kDa. Assuming adduct formation between the proteins, the new peak can be assigned as  $\sim\text{Au}_{36}@\text{BSA-Lyz}$ . Peak position remained the same after 24 h as well as 48 h of incubation indicating the formation of a stable species in the solution. The possibility of formation of  $\text{Au}_{36}$  in monolayer protected clusters has been reported earlier.<sup>10</sup> In the lower mass region (<20 kDa), a few Au attachments were observed with Lyz along with the fragments of BSA and Lyz (Fig. S2).

### 3.2. Identification of mixed protein aggregates by MALDI MS

In order to check the formation of BSA-Lyz adducts in the reaction conditions, several control experiments were performed and the presence of this species was verified using MALDI MS. The mass spectra of i) pure BSA, ii)  $\text{Au}^+$ -BSA adduct, iii) Lyz, iv)  $\text{Au}^+$ -Lyz adduct, v) BSA and Lyz mixture in presence of NaOH and vi) BSA and Lyz mixture are shown in Fig. 2. Molecular ion peak of BSA appears at 66.7 kDa as shown in the spectrum i). Corresponding doubly charged species at 33.3 kDa was also observed. Beyond 66.7 kDa, only the dimer of BSA was observed at 133.4 kDa and no peak was observed in the mass range of 70-100 kDa. Once  $\text{Au}^{3+}$  was added to the BSA solution, the main protein peak was

shifted by 3.2 kDa as shown in ii) and the resulting adduct was assigned as  $\sim\text{Au}_{16}\text{-BSA}$ . In this state, Au is in +1 oxidation state (as revealed by X-ray photoelectron spectroscopy).<sup>31</sup> Monomer of Lyz shows a peak at  $m/z$  14.3 kDa and the corresponding doubly charged species was observed at  $m/z$  7.2 kDa. Lyz is known to form aggregates in solution and a maximum up to hexamer of individual protein was observed in the mass range studied. Corresponding dimer, trimer and tetramer peaks were observed at  $m/z$  28.6, 42.9 and 57.2 kDa, respectively (Fig. S3). Pentamer and hexamer were observed at  $m/z$  71.5 and 85.8 kDa, respectively as shown in iii). Beyond this the peak intensity was not significant.  $\text{Au}^+\text{-Lyz}$  adduct showed multiple Au attachments to the protein monomer as well as to the aggregates. The peaks were separated by  $m/z$  197 due to Au and maximum up to 10 Au attachments to Lyz were observed (Fig. S4). In the lower mass range, gas phase bare clusters were observed, which were reported earlier.<sup>35</sup> When BSA was mixed with Lyz, several possibilities exist

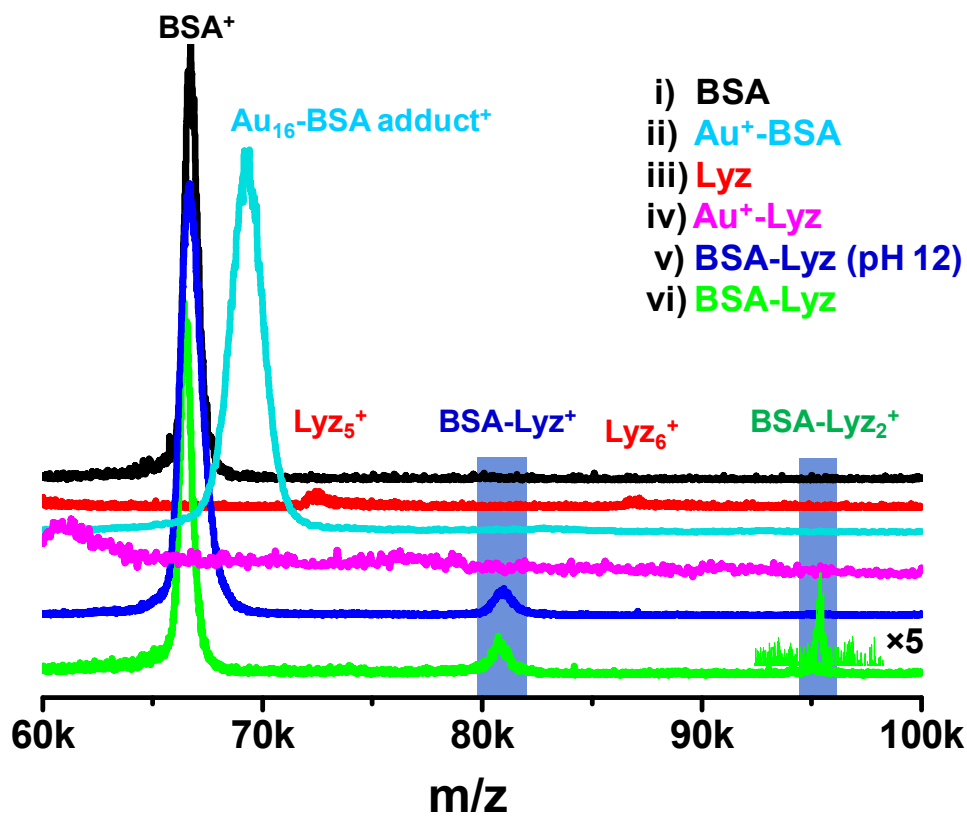


**Fig. 2.** MALDI MS of individual proteins, mixture of both the proteins and gold conjugate of individual proteins, showing formation of BSA-Lyz<sub>n</sub> (n = 0, 1, 2) conjugate.

like Lyz<sub>m</sub> (m = 1, 2, 3, 4), BSA<sub>n</sub> (n = 1, 2) and Lyz<sub>m</sub>BSA<sub>n</sub> (m = 1, 2; n = 1, 2). All these species were identified in MS in the higher mass region (m/z 80-150 kDa). Two distinct peaks were observed at m/z 81.0 kDa and 95.3 kDa, which appear to be spaced successively at 14.3 kDa from the BSA peak (m/z 66.7 kDa). Similar 14.3 kDa separation was observed for BSA dimer region (Fig. S5) beyond which, due to poor resolution and reduced intensity, we could not resolve other peaks. This separation clearly indicates the possibility of adduct formation between BSA and Lyz. This adduct formation can be explained in terms of aggregation tendency of Lyz. As we have mentioned earlier, Lyz forms aggregates and those can be seen in both MALDI and ESI MS.<sup>34</sup>

### 3.3. Spectroscopic and microscopic characterizations

Presence of Au along with C, O, N, S, Na and Cl was confirmed from the SEM/EDS spectrum. Around 1:2 Au:S ratio (atomic%) was observed in this case. Elemental mapping of AuM and SK indicated uniform distribution of Au throughout the protein. The presence of cluster in both the proteins (~Au<sub>36</sub>@BSA-Lyz) is further confirmed by XPS analysis which shows the presence of a metallic core (Fig. 3E). Au 4f<sub>7/2</sub> peak appears at 84.1 eV which shows the existence of zero valent state of the metal. Similar binding energy was observed for Au<sub>25</sub>@Lf.<sup>31</sup> Time dependent XPS study during the cluster formation and the corresponding MALDI MS data has been reported by Chaudhari *et al.* where they have shown how a protein-metal complex converts to zero valent state form during cluster formation and appearance of brown colour after the addition of reducing agent also indicates the reduction of the metal precursor during the cluster formation.<sup>31</sup> The S2p<sub>1/2</sub> peak at 163.3 eV (Figure S6)

confirms Au-S bonding, through the cysteine residues of the proteins. Protein protected clusters do not show well defined absorption

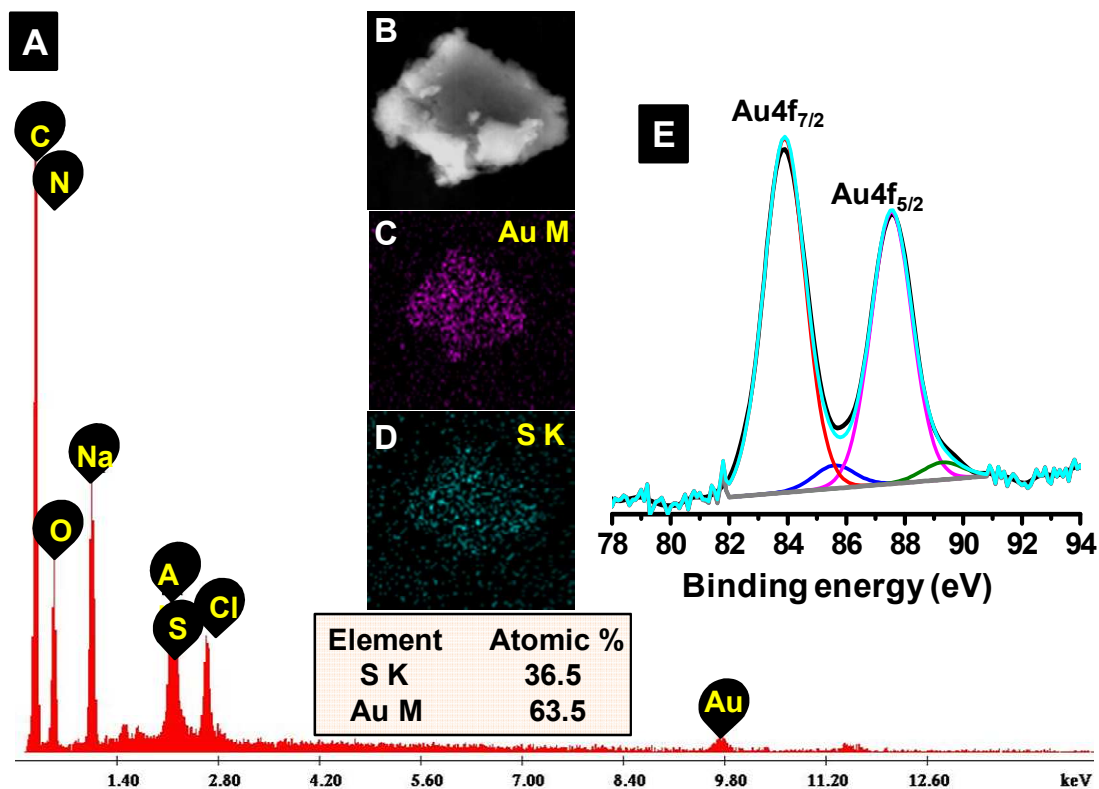


**Fig. 3.** (A) The SEM/EDAX spectrum of  $\sim\text{Au}_{36}\text{@BSA-Lyz}$  along with quantification data. (B) SEM image of a cluster sample. (C-D) EDAX images of the same showing the presence of Au and S. (E) XPS spectrum of  $\sim\text{Au}_{36}\text{@BSA-Lyz}$  confirms the presence of gold in the metallic state.

features like monolayer protected clusters. Although the UV/Vis technique is not useful to know the size of the cluster in protein systems, it helps to rule out the possibility of the presence of plasmonic nanoparticles in the solution. UV/Vis spectra show a peak at  $\sim 280$  nm which is due to presence of aromatic amino acid groups in protein systems (Fig. S7). In the case of  $\sim\text{Au}_{36}\text{@BSA-Lyz}$ , a similar type of absorption feature was observed at 280 nm. In

addition, a broad hump was observed at 510 nm which was not observed before for any such protein protected clusters.

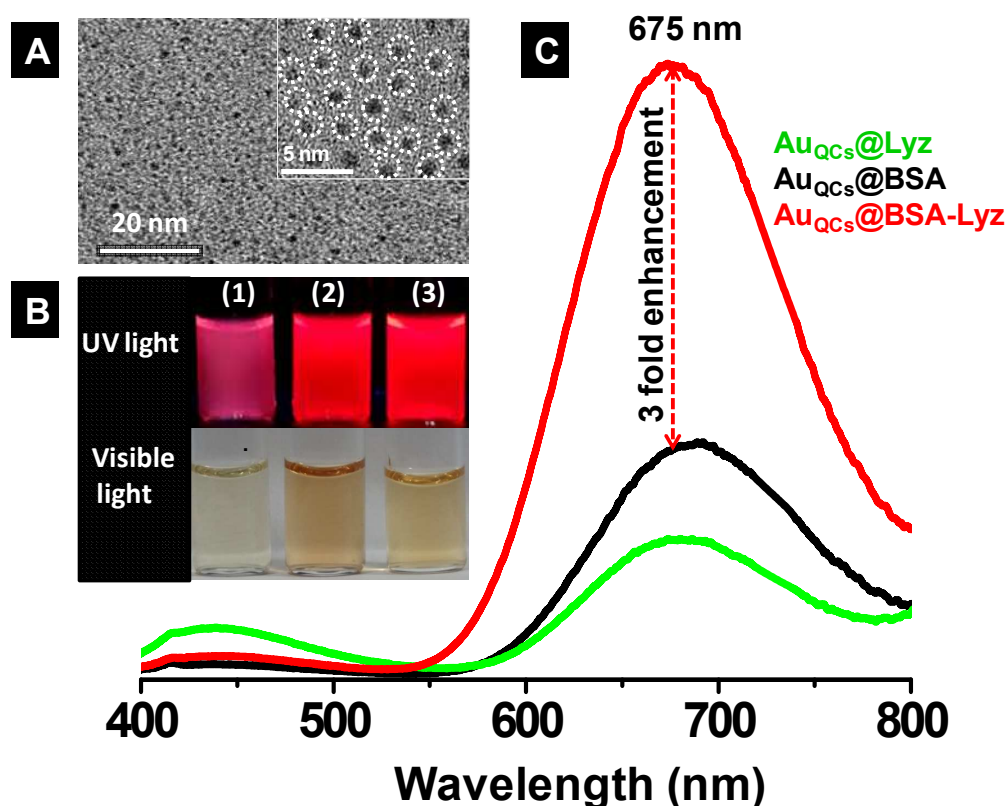


**Fig. 4.** (A) HRTEM image of Au<sub>QC</sub>@BSA-Lyz shows a core size of  $1.2 \pm 0.1$  nm. Expanded view is shown in the inset. Some of the clusters are shown in circle. (B) Photographs of Au<sub>10</sub>@Lyz (1), Au<sub>30</sub>@BSA (2) and Au<sub>QC</sub>@BSA-Lyz (3) under UV and visible light, respectively. (C) About 3 times enhancement in emission intensity of Au<sub>QC</sub>@BSA-Lyz compared to clusters protected by single proteins was seen, when excited at the same wavelength and at the same metal and protein concentrations.

HRTEM analysis of the new cluster showed the core size to be about 1.2 nm as shown in Fig. 4A. However, investigation of the cluster size through HRTEM analysis is not accurate as electron beam induces the growth of clusters in such soft materials. But this technique helps in knowing the approximate size of the samples. Since this is high resolution instrument with

point to point resolution of 0.12 nm, the approximate size is  $1.2 \pm 0.1$  nm. In the present study, this technique showed the absence of bigger plasmonic nanoparticles in the sample. It is important to note that the size of the new species in both these proteins ( $\sim\text{Au}_{36}@\text{BSA-Lyz}$ ) is similar as in the case of individual protein protected clusters. No bigger nanoparticle was found in TEM. Absence of plasmonic peak in the absorption spectrum also supports the HRTEM data. The photographs of  $\sim\text{Au}_{36}@\text{BSA-Lyz}$  along with individual protein protected clusters under UV as well as visible light are shown in Fig. 4 B.

### 3.4. Enhanced photoluminescence and mechanism of cluster formation

The photoluminescence spectra of parent clusters along with  $\sim\text{Au}_{36}@\text{BSA-Lyz}$  are shown Fig. 4C. The emission intensity of  $\sim\text{Au}_{36}@\text{BSA-Lyz}$  showed three and four fold enhancement than individual  $\text{Au}_{10}@\text{Lyz}$  and  $\sim\text{Au}_{30}@\text{BSA}$ , respectively when all the clusters were excited at 365 nm keeping the overall protein concentration the same for all the cases. The calculated quantum yield of  $\sim\text{Au}_{36}@\text{BSA-Lyz}$  was 42.4% considering rhodamine 6G as the reference, which is extremely high compared to all the reported gold clusters in various proteins. In similar experimental conditions, the quantum yield of  $\text{Au}_{\text{QC}}@\text{BSA}$  and  $\text{Au}_{\text{QC}}@\text{Lyz}$  were found to be 10.0% and 15.0%, respectively. These values are comparable to the ones reported.<sup>34</sup> Like other protein protected clusters, two excitation peaks were observed in the present study, one due to the cluster core (500 nm) and the other due to the protein (365 nm). Both the excitation maxima resulted in the same emission but with different intensity. Higher intensity was observed with 365 nm excitation which was explained in terms of FRET. Muhammed *et al.* have shown metal enhanced luminescence of  $\text{Au}_{\text{QC}}@\text{BSA}$  in presence of silver nanoparticles where protein shell acts as a spacer between the cluster and silver nanoparticles.<sup>23</sup> Distance between the fluorophore and the metal surface plays an important role in luminescence enhancement. Aggregation induced enhanced luminescence of Au(I) thiolate has been reported by Luo *et al.* where they have shown that Au(I) thiolate

shell surrounding the Au(0) core increased the luminescence drastically.<sup>51</sup> Wang *et al.* have shown a 200 fold increase in luminescence by replacing silver atoms with gold cluster.<sup>50</sup> In our case, increased emission intensity can be explained considering a FRET possibility between the cluster core and the two proteins. As discussed earlier (in the section on mass spectrometry), the cluster core is protected with two proteins which implies that both the proteins are in proximity for energy transfer and hence enhancement in FRET occurs. Here protein can be FRET donor and cluster can be the acceptor. In order to know whether the excess protein can also increase FRET activity, we have added different volumes of BSA to  $\sim\text{Au}_{30}@BSA$  solution. No significant increase in PL intensity was observed confirming that inter-protein energy transfer is not efficient in this case. Similar observations were made for  $\text{Au}_{QC}@Lyz$  also. Time dependent PL did not exhibit any change in the position of the emission.

As shown in Figure 1, mixed aggregates of BSA and Lyz are also capable of forming clusters and the cluster was assigned as  $\sim\text{Au}_{36}@BSA-Lyz$ . In one possibility, the cluster can form inside one protein (namely BSA, as it is large and can accommodate the 36-atom core) and the other protein, Lyz forms aggregate with the as-formed BSA protected cluster. Another possibility could be the formation of the cluster in the solution and then subsequent protection by both the proteins. In the case of a mixture of proteins in the Lyz region, only 5-6 Au separations from the parent protein peak was observed, while in the BSA region, the  $\text{Au}_{30}@BSA$  species was seen. However, another peak, observed at 88.2 kDa could be due to the separation of 36 Au from the BSA-Lyz adduct. To understand the mechanism of formation, we have added different volumes of Lyz to  $\sim\text{Au}_{30}@BSA$  and monitored the change by MS. After addition, each sample was stirred for 6 h and spotted for MALDI MS. In the Lyz region, only intensity enhancement with increase in Lyz concentration was observed but no cluster formation occurred in this situation. In the BSA region, a decrease in

core nuclearity with the addition of Lyz was observed in the system. Two humps separated by 5 Au and 16 Au from the parent BSA (initially the separation was 30 Au) along with appearance of free BSA were observed. The peak positions were the same for all the concentrations of Lyz used. New humps corresponding to BSA-Lyz,  $\text{Au}_8\text{@BSA-Lyz}$  and  $\sim\text{Au}_{23}\text{@BSA-Lyz}$  were observed. However, due to poor intensity, peak assignments may vary slightly.

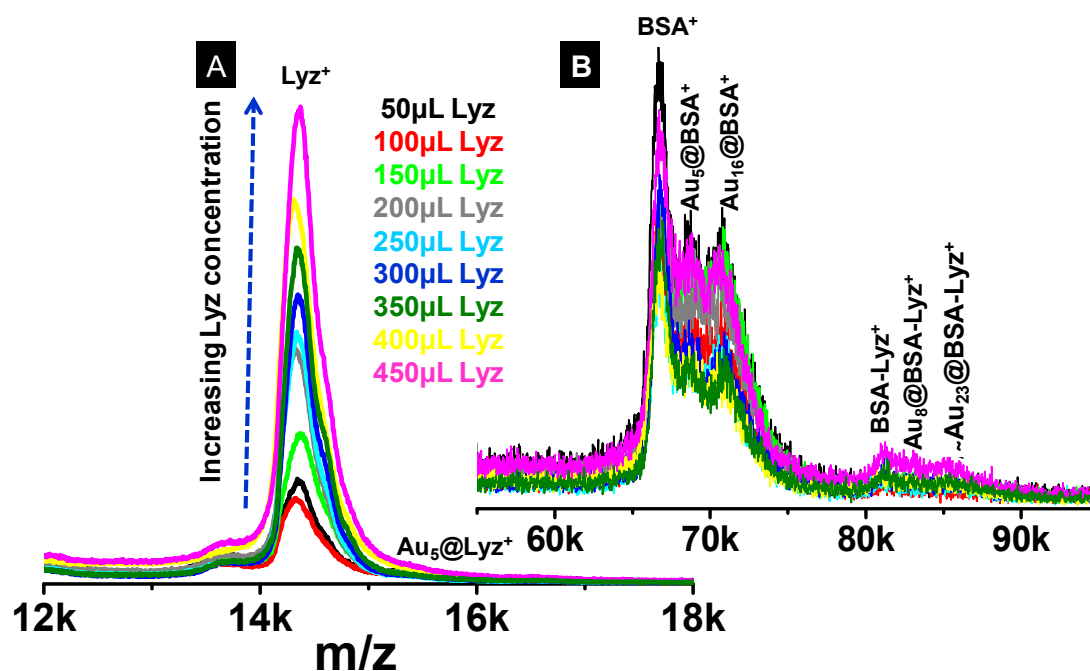


**Fig. 5.** Different volumes of Lyz solution (75µM) were added to preformed  $\text{Au}_{\text{QCs}}\text{@BSA}$  with regular increase in 50µL. No mass shift was observed in the Lyz region other than increase in Lyz peak intensity as shown in A. The Lyz peak has a shoulder and that may be due to few Au attachments. The main cluster peak in the BSA region splits into two small humps separated by 5 Au and 16 Au from the parent BSA peak. BSA-Lyz adduct and  $\text{Au}_8\text{@BSA-Lyz}$  and  $\sim\text{Au}_{23}\text{@BSA-Lyz}$  were observed in the higher mass spectral region.

In this study, large protein-large protein interaction was also considered. For this, lactoferrin (Lf) of m/z 83.0 kDa was chosen. Gold clusters protected by BSA as well as by Lf are



already reported and are well characterized by mass spectrometry.  $\text{Au}_{\text{QC}}@\text{BSA}^{27}$  and  $\text{Au}_{\text{QC}}@\text{Lf}^{32}$  were synthesized according to a previously reported method. When both  $\text{Au}_{\text{QC}}@\text{BSA}$  and  $\text{Au}_{\text{QC}}@\text{Lf}$  were mixed together, maintaining certain conditions, no distinct features were observed other than the individual cluster peak in the whole mass spectral range. Different control experiments were also carried out (as mentioned above) to check the interaction of both the proteins separately and those along with protein protected clusters. But in none of the cases new features were observed which could be due to the bulky nature of the proteins, which restricts them to form inter-protein adducts.

### 3.5. Silver clusters

Similar studies were also performed for Ag clusters where we have observed concentration dependent growth in the cluster core. For a similar concentration of Ag precursor,  $\sim\text{Ag}_{28}@\text{BSA}$  and  $\sim\text{Ag}_{35}@\text{BSA-Lyz}$  were observed. In the Lyz region, 8 Ag attachments to Lyz were observed. We have performed concentration-dependent study by varying the silver

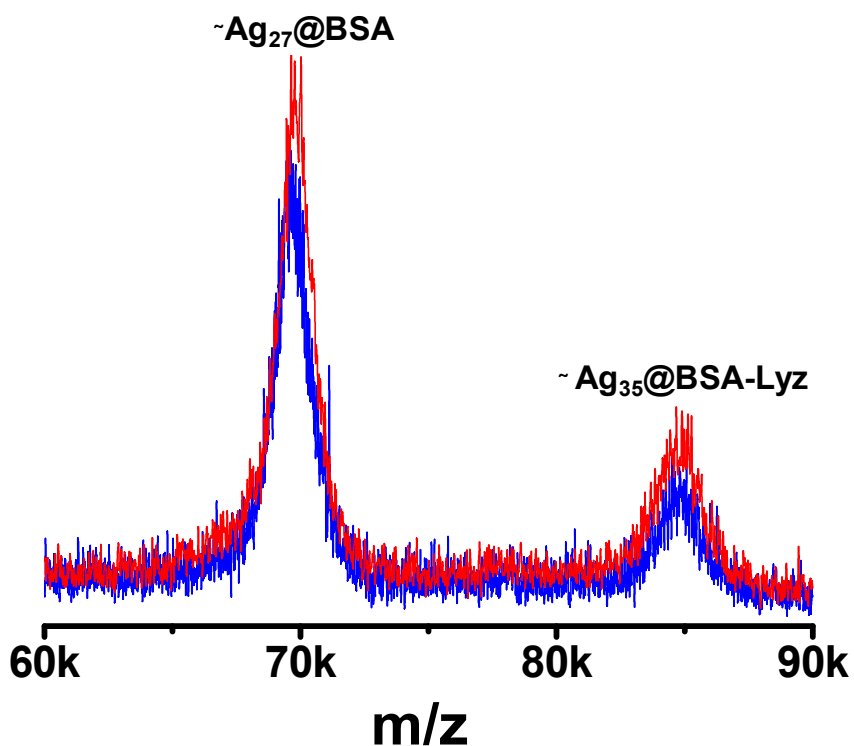


**Fig. 6.** Time dependent MALDI MS study on Ag system which shows the formation of  $\sim\text{Ag}_{35}\text{@BSA-Lyz}$  along with the individual cluster peak. The peak positions as well as peak intensity are the same with time (blue line (after 12 h) and red line (after 24 h)).

concentration (final concentration was 2, 3 and 4 mM) keeping protein concentration the same.  $\sim\text{Ag}_{16}\text{@BSA}$  and  $\sim\text{Ag}_{28}\text{@BSA}$  and  $\sim\text{Ag}_{34}\text{@BSA}$  were observed for 2, 3 and 4 mM Ag concentration, respectively in the BSA region. Similar mass shift with respect to Ag concentration was also reflected in the mixed protein adduct mass region where  $\sim\text{Ag}_{25}\text{@BSA-Lyz}$ ,  $\sim\text{Ag}_{35}\text{@BSA-Lyz}$  and  $\sim\text{Ag}_{42}\text{@BSA-Lyz}$  were observed for 2, 3 and 4 mM Ag, respectively (Fig. S8). XPS analysis of this system also showed the presence of metallic silver core where Ag is in  $\text{Ag}^0$  state. In this case also increased emission intensity, comparable with Au was observed.

By comparing the data obtained for Au and Ag, it can be seen that the mass shift is always more in the mixed protein than in the individual protein. For similar concentration of Au and Ag, Au<sub>30</sub> and Ag<sub>26</sub> cores can be achieved, protected by BSA alone. The other peak (at higher mass range) was shifted by 36 Au and 35 Ag from the combined mass of BSA and Lyz. If the probabilities mentioned above are narrowed down, only two possibilities exist; i)  $\sim\text{Au}_{30}/\text{Ag}_{27}@\text{BSA}+\text{Au}_6/\text{Ag}_8@\text{Lyz}$  or ii)  $\sim\text{Au}_{36}/\text{Ag}_{35}@\text{BSA}+\text{Lyz}$ . Considering PL data along with mass spectral finding, a four-fold enhancement in emission intensity (in case of Au) was observed which can be attributed to the presence of multiple cluster cores in the system which increases the probability of FRET. In the other case, where we consider the presence of a single core protected by multiple protein, proximity of two different proteins attached to a single core can also enhance FRET efficiently. From the TEM, pairs of clusters separated by a couple of nanometers are not seen, which would support a single cluster core. While consequent decrease in the nuclearity of the cluster appears to suggest the multiple core idea. Thus the mechanism requires further investigation which can be resolved only by crystallization of all the species.

#### 4. Summary and Conclusion

In summary, we have demonstrated the synthesis of Au clusters protected by mixed protein systems with high quantum yield. Such clusters were prepared by mixing Au<sup>3+</sup> with mixture of both the proteins and then subsequently reduced to Au<sup>0</sup> at pH 12. On the basis of MALDI MS, it is assigned as  $\sim\text{Au}_{36}@\text{BSA}-\text{Lyz}$ . Similar observations were also made for the silver system,  $\sim\text{Ag}_{35}@\text{BSA}-\text{Lyz}$ . The existence of mixed proteins in the form of adduct was confirmed by extensive mass spectral investigations and control studies. XPS analysis revealed that the Au cluster protected by the mixed protein system is in zero valent state. HRTEM analysis of these clusters showed the core size is about 1.2 nm which is in agreement with the size of clusters protected by individual proteins. A fourfold enhancement

in the emission intensity of  $\sim\text{Au}_{36}@\text{BSA-Lyz}$  was observed, compared to the individual clusters when excited at the same wavelength. The quantum yield of  $\sim\text{Au}_{36}@\text{BSA-Lyz}$  was found to be 42.4% which is extremely high compared to the already reported clusters. Proximity of two different proteins around a core can enhance FRET and hence the emission intensity. Presence of multiple cluster species in solution or cluster protected by mixed protein systems might be another reason for such a high quantum yield. Understanding the system in detail is limited by several factors. Separation of the specific entity from the mixture of free proteins and other clusters can help to understand the system in greater detail. Similarly studies like SAXS and spectroscopy may help to understand the system in more detail, which is part of our future investigations. Such a kind of system can be used for sensing ultralow levels of analytes, in view of the sensitivity of protein protected clusters to a range of analytes. Being bio-compatible, these can be used as fluorescent tags and can replace fluorescent dyes for staining biological entities and tracking biomolecules in real systems.

### Supporting Information

Comparative MALDI MS of BSA and  $\sim\text{Au}_{30}@\text{BSA}$  at higher and lower mass range, MALDI MS of Lyz and  $\text{Au}^+\text{-Lyz}$ , BSA-Lyz adducts, XPS survey spectrum, UV-vis spectra, concentration dependent MALDI MS of  $\text{Ag}_{\text{QC}}@\text{BSA-Lyz}$  are available in the Supplementary Information.

### Author Information

\*Corresponding Author: T. Pradeep, Email: [Pradeep@iitm.ac.in](mailto:Pradeep@iitm.ac.in), Fax: +91-44-2257-0545.

### Acknowledgements:

A.B., J.S.M. and T.P. thank the Department of Science and Technology, Government of India for continuous support of our research program on nanomaterials. A.B. thanks the Council of

Scientific and Industrial Research (CSIR) for fellowship. J. S. M. thanks IIT Madras for a fellowship. T.P. and H.L. thank the India-Korea research program for a joint project.

## Reference

1. R. Jin, *Nanoscale*, 2010, **2**, 343-362.
2. A. Mathew and T. Pradeep, *Part. Part. Syst. Charact.*, 2014, n/a-n/a.
3. T. Udayabhaskararao and T. Pradeep, *J. Phys. Chem. Lett.*, 2013, **4**, 1553-1564.
4. P. L. Xavier, K. Chaudhari, A. Baksi and T. Pradeep, *Nano Rev.*, 2012, **3**, 14767 and the references cited there in.
5. D. M. Chevrier, A. Chatt and P. Zhang, *J. Nanophoton.*, 2012, **6**, 064504-064501-064504-064516.
6. M. W. Heaven, A. Dass, P. S. White, K. M. Holt and R. W. Murray, *J. Am. Chem. Soc.*, 2008, **130**, 3754-3755.
7. M. Zhu, C. M. Aikens, F. J. Hollander, G. C. Schatz and R. Jin, *J. Am. Chem. Soc.*, 2008, **130**, 5883-5885.
8. D. Crasto, S. Malola, G. Brosofsky, A. Dass and H. Hakkinen, *J. Am. Chem. Soc.*, 2014, **136**, 5000-5005.
9. H. Qian, W. T. Eckenhoff, Y. Zhu, T. Pintauer and R. Jin, *J. Am. Chem. Soc.*, 2010, **132**, 8280-8281.
10. C. Zeng, H. Qian, T. Li, G. Li, N. L. Rosi, B. Yoon, R. N. Barnett, R. L. Whetten, U. Landman and R. Jin, *Angew. Chem. Int. Ed.*, 2012, **51**, 13114-13118.
11. P. D. Jadzinsky, G. Calero, C. J. Ackerson, D. A. Bushnell and R. D. Kornberg, *Science*, 2007, **318**, 430-433.
12. H. Yang, Y. Wang, H. Huang, L. Gell, L. Lehtovaara, S. Malola, H. Häkkinen and N. Zheng, *Nat. Commun.*, 2013, **4**.
13. A. Desireddy, B. E. Conn, J. Guo, B. Yoon, R. N. Barnett, B. M. Monahan, K. Kirschbaum, W. P. Griffith, R. L. Whetten, U. Landman and T. P. Bigioni, *Nature*, 2013, **501**, 399-402.
14. J. Hassinen, P. Pulkkinen, E. Kalenius, T. Pradeep, H. Tenhu, H. Hakkinen and R. H. A. Ras, *J. Phys. Chem. Lett.*, 2014, **5**, 585-589.
15. A. Mathew, G. Natarajan, L. Lehtovaara, H. Hakkinen, R. M. Kumar, V. Subramanian, A. Jaleel and T. Pradeep, *ACS Nano*, 2014, **8**, 139-152.
16. Y. Niihori, M. Matsuzaki, T. Pradeep and Y. Negishi, *J. Am. Chem. Soc.*, 2013, **135**, 4946-4949.
17. T. Pradeep, A. Baksi and P. L. Xavier, in *Functional Nanometer-Sized Clusters of Transition Metals: Synthesis, Properties and Applications*, The Royal Society of Chemistry, 2014, pp. 169-225.
18. N. Goswami, K. Zheng and J. Xie, *Nanoscale*, 2014, **6**, 13328-13347.
19. J. T. Petty, J. Zheng, N. V. Hud and R. M. Dickson, *J. Am. Chem. Soc.*, 2004, **126**, 5207.
20. J. Zheng, C. Zhang and R. M. Dickson, *Phys. Rev. Lett.*, 2004, **93**, 077402/077401-077404.
21. J. Xie, Y. Zheng and J. Y. Ying, *J. Am. Chem. Soc.*, 2009, **131**, 888-889.
22. L. Shang, Y. Wang, J. Jiang and S. Dong, *Langmuir*, 2007, **23**, 2714-2721.
23. M. A. Habeeb Muhammed, P. K. Verma, S. K. Pal, A. Retnakumari, M. Koyakutty, S. Nair and T. Pradeep, *Chem. - Eur. J.*, 2010, **16**, 10103-10112.
24. Y. Liu, K. Ai, X. Cheng, L. Huo and L. Lu, *Adv. Funct. Mater.*, 2010, **20**, 951-956.
25. A. Mathew, P. R. Sajanlal and T. Pradeep, *J. Mater. Chem.*, 2010, **21**, 11205-11212.
26. J. Xie, Y. Zheng and J. Y. Ying, *Chem. Commun.*, 2010, **46**, 961-963.
27. J. S. Mohanty, P. L. Xavier, K. Chaudhari, M. S. Bootharaju, N. Goswami, S. K. Pal and T. Pradeep, *Nanoscale*, 2012, **4**, 4255-4262.
28. H.-W. Li, K. Ai and Y. Wu, *Chem. Commun.*, 2011, **47**, 9852-9854.
29. U. Anand, S. Ghosh and S. Mukherjee, *J. Phys. Chem. Lett.*, 2012, **3**, 3605-3609.
30. P.-H. Chan and Y.-C. Chen, *Anal. Chem.*, 2012, **84**, 8952-8956.

31. K. Chaudhari, P. L. Xavier and T. Pradeep, *ACS Nano*, 2011, **5**, 8816-8827.
32. P. L. Xavier, K. Chaudhari, P. K. Verma, S. K. Pal and T. Pradeep, *Nanoscale*, 2010, **2**, 2769-2776.
33. H. Wei, Z. Wang, L. Yang, S. Tian, C. Hou and Y. Lu, *Analyst* 2010, **135**, 1406-1410.
34. A. Bakshi, P. L. Xavier, K. Chaudhari, N. Goswami, S. K. Pal and T. Pradeep, *Nanoscale*, 2013, **5**, 2009-2016.
35. A. Bakshi, T. Pradeep, B. Yoon, C. Yannouleas and U. Landman, *ChemPhysChem*, 2013, **14**, 1272-1282 and the references cited there in.
36. A. Bakshi and T. Pradeep, *Nanoscale*, 2013, **5**, 12245-12254.
37. C.-L. Liu, H.-T. Wu, Y.-H. Hsiao, C.-W. Lai, C.-W. Shih, Y.-K. Peng, K.-C. Tang, H.-W. Chang, Y.-C. Chien, J.-K. Hsiao, J.-T. Cheng and P.-T. Chou, *Angew. Chem., Int. Ed.*, 2011, **50**, 7056-7060.
38. Y. Yu, Z. Luo, C. S. Teo, Y. N. Tan and J. Xie, *Chem. Commun.*, 2013, **49**, 9740-9742.
39. H.-Y. Liu, X. Zhang, X.-M. Wu, L.-P. Jiang, C. Burda and J.-J. Zhu, *Chem. Commun.*, 2011, **47**, 4237.
40. Y. Yue, T.-Y. Liu, H.-W. Li, Z. Liu and Y. Wu, *Nanoscale*, 2012, **4**, 2251-2254.
41. L. Yan, Y. Cai, B. Zheng, H. Yuan, Y. Guo, D. Xiao and M. M. F. Choi, *J. Mater. Chem.*, 2012, **22**, 1000-1005.
42. T.-H. Chen and W.-L. Tseng, *Small*, 2012, **8**, 1912-1919.
43. G. Guan, S.-Y. Zhang, Y. Cai, S. Liu, M. S. Bharathi, M. Low, Y. Yu, J. Xie, Y. Zheng, Y.-W. Zhang and M.-Y. Han, *Chem. Commun. (Cambridge, U. K.)*, 2014, **50**, 5703-5705.
44. S. D. Haveli, P. Walter, G. Patriarche, J. Ayache, J. Castaing, E. E. Van, G. Tsoucaris, P.-A. Wang and H. B. Kagan, *Nano Lett.*, 2012, **12**, 6212-6217.
45. M. Li, D.-P. Yang, X. Wang, J. Lu and D. Cui, *Nanoscale Res. Lett.*, 2013, **8**, 182.
46. C. Shao, B. Yuan, H. Wang, Q. Zhou, Y. Li, Y. Guan and Z. Deng, *J. Mater. Chem.*, 2011, **21**, 2863.
47. X. Wen, P. Yu, Y.-R. Toh, A.-C. Hsu, Y.-C. Lee and J. Tang, *J. Phys. Chem. C*, 2012, **116**, 19032-19038.
48. X. Xia, Y. Long and J. Wang, *Anal. Chim. Acta*, 2013, **772**, 81-86.
49. M. A. H. Muhammed and T. Pradeep, in *Advanced Fluorescence Reporters in Chemistry and Biology II*, ed. A. P. Demchenko, Springer Berlin Heidelberg, 2010, pp. 333-353.
50. S. Wang, X. Meng, A. Das, T. Li, Y. Song, T. Cao, X. Zhu, M. Zhu and R. Jin, *Angew. Chem., Int. Ed.*, 2014, **53**, 2376-2380.
51. Z. Luo, X. Yuan, Y. Yu, Q. Zhang, D. T. Leong, J. Y. Lee and J. Xie, *J. Am. Chem. Soc.*, 2012, **134**, 16662-16670.

## Table of Content

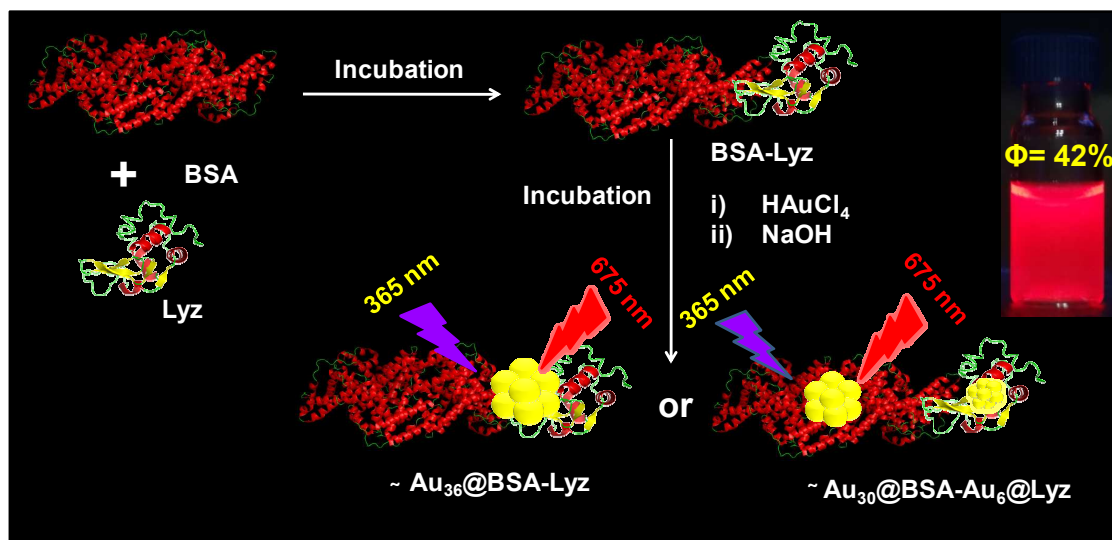


**Table of Content Text:** Noble metal clusters in mixed protein (BSA-Lyz) matrix lead to better FRET and high fluorescence quantum yield.